Enhancement patterns of intrahepatic mass-forming cholangiocarcinoma at multiphasic computed tomography and magnetic resonance imaging and correlation with clinicopathologic features

M. CIRESA¹, A.M. DE GAETANO¹, M. POMPILI², A. SAVIANO², A. INFANTE¹, M. MONTAGNA², A. GUERRA¹, M. GIUGA¹, M. VELLONE³, F. ARDITO³, A. DE ROSE³, F. GIULIANTE³, F.M. VECCHIO⁴, A. GASBARRINI², L. BONOMO¹

Abstract. – OBJECTIVE: Incidence of intrahepatic mass-forming cholangiocarcinoma (IMCC) is increasing worldwide, especially in patients with chronic liver disease. The small and the histologically well-differentiated IMCCs in chronic liver disease could be arterially hypervascular lesions with/without washout on computed tomography (CT) and magnetic resonance imaging (MRI), mimicking typical hepatocellular carcinoma (HCC). The aim of this work is to evaluate contrast enhancement (CE) patterns of IMCCs at quadri-phasic multidetector CT (4-MDCT) and MRI, using imaging-clinicopathologic correlation.

PATIENTS AND METHODS: The 4-MDCT and MR images of 56 histologically confirmed IMCCs were retrospectively evaluated for tumor morphology and enhancement features. Enhancement pattern was defined according to the behavior of the nodule in arterial (AP), portal venous (PVP) and equilibrium phases (EP), and dynamic pattern was described according to enhancement progression throughout the different phases. Arterial and dynamic enhancement patterns were correlated with chronic liver disease, tumor size and histological differentiation.

RESULTS: Most of the nodules were peripherally hyperenhancing (50%) on AP, and partially hyperenhancing on PVP (67.9%) and EP (80.3%). Forty-six (82.1%) IMCCs showed progressive CE, 7 (12.5%) stable CE and 3 (5.4%) wash-out. In

normal liver there were 34 nodules with progressive and 3 with stable CE, whereas in chronic liver disease there were 12 IMCCs with progressive, 4 with stable and 3 with washout pattern (p = 0.01); IMCCs with progressive CE were more differentiated than IMCCs with stable CE and wash-out (p = 0.02).

CONCLUSIONS: The most prevalent enhancement pattern of IMCCs was arterial rim enhancement followed by progressive and concentric filling. The stable and the washout patterns were more frequent in poorly differentiated IMCCs. Contrast washout was observed only in IMCCs emerging in chronic liver disease with a risk of misdiagnosis with HCC.

Key Words:

Intrahepatic mass-forming cholangiocarcinoma, Multidetector computed tomography, Magnetic resonance imaging, Dynamic enhancement pattern, Chronic liver disease, Histological differentiation.

Introduction

Intrahepatic cholangiocarcinoma (ICC), a tumor with biliary tract differentiation pathologic features¹, is the second most common primary liver cancer worldwide after hepatocellular carcinoma (HCC), accounting for 15-20% of all pri-

¹Department of Bioimaging and Radiological Sciences, "Agostino Gemelli" Hospital, Catholic University of the Sacred Heart, School of Medicine, Rome, Italy

²Department of Internal Medicine, "Agostino Gemelli" Hospital, Catholic University of the Sacred Heart, School of Medicine, Rome, Italy

³Department of Surgery, "Agostino Gemelli" Hospital, Catholic University of the Sacred Heart, School of Medicine, Rome, Italy

⁴Department of Anatomo-Pathology, "Agostino Gemelli" Hospital, Catholic University of the Sacred Heart, School of Medicine, Rome, Italy

mary liver cancers²; the incidence of ICC is on the rise, especially in Western Countries, where may be as high as 2.1 per 100,000 person a year³.

More recently recognized risk factors for ICC are similar to those known for HCC, as cirrhosis of any cause, chronic viral hepatitis B or C⁴, obesity, diabetes and heavy alcohol consumption⁵ and this association may be the cause of the increasing incidence of ICC in recent years in patients with chronic liver disease. Recent data also indicate common genomic traits between ICC and HCC, supporting the hypothesis of common cell ancestors and common pathobiological pathways to all primary liver parenchymal tumours⁶.

The morphologic classification system for primary liver cancer proposed by the Liver Cancer Study Group of Japan divides ICC into three types based on macroscopic appearance: the mass-forming type, the periductal infiltrative type, and the intraductal growing type7. Massforming ICC (IMCC) is the most common type and shows a radial growth pattern, invading into the adjacent hepatic parenchyma. Close attention is required to differentiate IMCC from HCC because prognosis and treatment options differ significantly; distinct imaging features of IMCC and HCC are well documented in literature therefore accurate diagnosis of these two entities is possible in most cases⁸⁻¹². IMCC typically shows initial rim enhancement, followed by progressive and concentric filling with contrast material at dynamic computed tomography (CT) or magnetic resonance imaging (MRI); this effect may reflect fibrosis which is slow to enhance but retains the intravenous contrast agent. In contrast, HCC enhances more intensely than the surrounding liver in the arterial phase (AP) while it enhances less than the surrounding liver in the equilibrium phase (EP); the presence of arterial uptake followed by washout is highly specific for HCC and this dynamic pattern is the current non-invasive diagnostic criteria for HCC proposed by the American Association for the Study of Liver Disease (AASLD)¹³ and by the European Association for the Study of the Liver and the European Organisation for Research and Treatment of Cancer (EASL-EORTC)¹⁴. Recent guidelines for the diagnosis and management of ICC proposed by EASL¹⁵, established that a pathological diagnosis is required for a definitive diagnosis of ICC, while a presumed radiographic diagnosis of ICC is sufficient in the absence of other extrahepatic primary malignancies and cirrhosis if a decision has been made to proceed

with surgical resection. Currently, radiological studies cannot reliably differentiate between scirrhous HCC and IMCC, or metastatic adenocarcinoma and IMCC¹⁶. On the other hand, recent studies showed that IMCC in cirrhosis patients can also display intense contrast uptake during the AP followed by washout on liver contrast enhanced ultrasonography^{17,18}. Therefore, only 4phase (unenhanced, arterial, portal venous and equilibrium phases) multidetector CT (MDCT) or dynamic contrast enhanced MRI are recommended for non-invasive diagnosis of HCC^{13,14}. However, several recent reports demonstrated that IMCC, particularly the small (< 3 cm in diameter) and the histologically well-differentiated lesions in chronic liver disease could show an atypical enhancement pattern as an arterially hyperenhancing lesion with/without washout on CT and MRI, mimicking HCC¹⁹⁻²⁴; therefore the non-invasive diagnostic criteria for HCC proposed by EASL-EORTC and by AASLD could be questioned.

The purpose of this work was to retrospectively evaluate enhancement patterns of IMCC at 4-MDCT or dynamic MRI and to correlate the arterial and dynamic enhancement features with chronic liver disease, tumour size and histological differentiation.

Patients and Methods

Patient Selection

We retrospectively searched our hospital's hepatocellular carcinoma multidisciplinary group database between January 2006 and June 2014 using the search terms intrahepatic cholangiocarcinoma. This search identified 108 patients. Those who met the following inclusion criteria were selected for our study: (a) pathologically confirmed diagnosis of IMCC on the basis of surgical resection or percutaneous biopsy, and (b) available 4-MDCT or dynamic contrast-enhanced liver MRI scans. Therefore, we excluded cases of hilar CC (n = 6), combined HCC-ICC (n = 3) and of IMCC without 4-MDCT or MRI images available (n = 43). In eleven patients with multiple nodules, only the larger lesion with histological confirmation was analysed. A total of 56 patients (mean age, 68.5 years; range, 25-89 years), including 31 men (mean age, 68 years; range, 25-89 years) and 25 women (mean age, 69 years; range, 44-87 years), were included in this study. The histological diagnosis of IMCC was confirmed at surgical resection (n = 34) or imageguided percutaneous biopsy (n = 22). Fifteen of these patients had liver cirrhosis due to hepatitis B virus (HBV, n = 3) or hepatitis C virus (HCV, n = 4) infection, alcohol abuse (n = 3), metabolic disorders (n = 1) or unknown cause (n = 4). In addition, four patients had chronic hepatitis due to B-viral infection (n = 1) or C-viral infection (n = 1), Caroli disease (n = 1) or unknown cause (n = 1). Chronic hepatitis and cirrhosis were confirmed by means of pathologic examination of liver biopsy in 9 patients and by means of unequivocal clinical and imaging criteria in the remaining 10 patients²⁵ (Table I).

Image Protocol

Thirty-four patients had undergone 4-MDCT, 12 patients had undergone dynamic contrast enhanced MRI, while both 4-MDCT and dynamic contrast enhanced MRI were performed for 10 patients.

CT technique – CT imaging was performed using 16- and 64-detector row CT scanners

Table I. Clinicopathological data of 56 patients with IMCC.

Characteristic	Value
Patients, No.	56
Age median (range), years	68.5 (25-89)
Gender, No. (%)	
Male	31 (55.4)
Female	25 (44.6)
Normal liver, No. (%)	37 (66)
Chronic liver disease (all causes), No. (%)	19 (34)
Chronic hepatitis, No. (%)	4 (7.2)
HBV, No.	1
HCV, No.	1
Other, No.	2
Liver cirrhosis, No. (%)	15 (26.8)
HBV, No.	3
HCV, No.	4
Alcohol, No.	3
Metabolic disorders, No.	1
Cryptogenetic, No.	4
Histological differentiation of tumors, No. (%)	
Gx	7 (12.5)
G1-G2	29 (51.8)
G3	20 (35.7)
Imaging techniques, No. (%)	
MDCT	34 (60.5)
MRI	12 (21.5)
MDCT + MRI	10 (18)

HBV: hepatitis B virus; HCV: hepatitis C virus; Gx: grade cannot be assessed; G1-G2: well-moderately differentiated; G3: poorly differentiated; MDCT: multidetector computed tomography; MRI: magnetic resonance imaging.

(Light Speed Plus, Ultra 16 and VCT; GE Medical Systems, Milwaukee, WI, USA). The parameters were as follows: detector collimation, 0.625-1.25 mm; table speed, 0.98-20 mm/s; gantry rotation time, 0.6-0.8 second; pitch, 0.5-1; section thickness, 2.5 mm; filter, standard; tube voltage, 120 KV; tube current, automA; and matrix, 512 x 512. Quadriphasic CT (unenhanced, arterial, portal venous and equilibrium phases) was performed; all patients underwent bolus intravenous injection of 2.0 ml/kg body weight of non-ionic contrast agent (iopromide - Ultravist 370 mgI/ml; Bayer HealthCare, Milan, Italy) through an 18gauge needle, followed by a 40-mL saline flush (0.9%) at a rate of 4 ml/s using a power injector (Medrad Stellant Dual Head Injector; Medrad, Warrendale, PA, USA). Bolus tracking software (SmartPrep; GE Medical Systems, Milwaukee, WI, USA) over the abdominal aorta near the celiac axis (threshold 120 HU) was used to time the AP. Scans started 10 s (AP) after reaching the threshold in the aorta, 70 s (portal venous phase, PVP) and 180 s (EP).

MRI technique – MRI was performed on a 1.5 T system (Signa Horizon; GE Medical Systems, Milwaukee, WI, USA) with a 8-channel phased-array body coil. The MRI baseline protocol included a breath-hold transverse T1weighted in-phase and opposed-phase 2D fast spoiled gradient-echo (2DFSPGR) sequence (TR/TE, 180/4.4-2.2; flip angle, 80°; FOV, 48 x 48 cm; matrix, 256 x 224; section thickness, 7 mm; slice spacing, 1 mm) a breath-hold transverse T2-weighted fast-recovery fast spinecho (FRFSE) sequence at two different echo times (TR/TE, 2050/80 and 140; eco train length, 17; FOV, 48 x 48 cm; matrix, 256 x 224; section thickness, 7 mm; slice spacing, 1 mm), with a frequency-selective fat suppression technique, a breath-hold transverse T2weighted fast spin-echo (FSE) sequence (TR/TE, 2200/84; eco train length, 17; FOV, 48 x 48 cm; matrix, 256 x 224; section thickness, 5 mm; slice spacing, 1 mm), a breathhold transverse T2-weighted single shot fast spin-echo (SSFSE) sequence (TR/TE, infinite/90; FOV, 48 x 48 cm; matrix, 256 x 256; section thickness, 6 mm; slice spacing, 1 mm), a breath-hold coronal T2-weighted single shot fast spin-echo (SSFSE) sequence (TR/TE, infinite/60; FOV, 48 x 48 cm; matrix, 256 x 192; section thickness, 4 mm; slice spacing 0). Dynamic imaging was performed after the administration of gadolinium-based contrast (gadobenate dimeglumine – MultiHance 0.50 mmol/ml; Bracco Diagnostics, Milan, Italy) at a dose of 0.1 mmol/kg body weight followed by a 20-mL saline flush (0.9%) with a 2.5mL/s flow rate, using a power injector (Medrad Spectris Solaris EP MR Injection System; Bayer Health Care, Milan, Italy). Imaging in the precontrast, AP (30 s), PVP (70 s) and EP (180 s) was performed using a T1weighted breath-hold transverse 3D fast spoiled gradient-echo (LAVA: Liver Acquisition with Volume Acceleration; GE Medical Systems, Milwaukee, WI, USA) sequence with fat suppression (TR/TE, 3.1/1.5; flip angle, 13°; bandwidth, 83.3 KHZ; FOV, 48 x 48 cm; matrix, 256 x 224; effective section thickness, 3.8 mm with no gap).

Imaging Interpretation

All CT and MR images were reviewed in consensus by two abdominal radiologists that were aware that IMCC had been diagnosed, but they were unaware of histological differentiation.

CT and MR scans were evaluated for their morphologic and enhancement features in stack mode at a picture archiving and communication systems workstation (Carestream Vue PACS version 11.4; Carestream Health Technology and Innovation Centre, Genoa, Italy). The attenuation and the signal intensity (SI) of each lesion were qualitatively evaluated.

For analysis of tumour enhancement features, the two radiologists determined the following: (a) the relative attenuation at CT or the relative SI at MRI of the lesion compared with that of the adjacent liver parenchyma; (b) the enhancement pattern of the lesion on AP, PVP and EP images; (c) the temporal changes in the degree of enhancement of the lesion during dynamic phase imaging. The relative attenuation and the relative SI of the lesion were compared with those of the surrounding liver parenchyma during unenhanced and enhanced phases; the lesions were recorded as hypoattenuating or hypointense, isoattenuating or isointense and hyperattenuating or hyperintense on unenhanced images and hypoenhancing, isoenhancing and hyperenhancing on enhanced images. Lesions that showed an inhomogeneous enhancement pattern on contrast-enhanced images were categorized according to the attenuation of the predominant parts of the lesions (>50%), as reported by Loyer et al11. After intravenous contrast administration, the enhancement through each of the different phases was registered as follows: (1) globally hyperenhancing: increased attenuation/SI, relative to the liver parenchyma, involving the totality of the lesion; (2) partially hyperenhancing: increased attenuation/SI involving more than 25% of the lesion; (3) peripherally hyperenhancing: increased attenuation/SI limited to the periphery of the lesion, involving less than 25% of its area, resembling a rim-like pattern; (4) isoenhancing: same attenuation/SI as the adjacent liver parenchyma; (5) hypoenhancing: lower attenuation/SI compared to hepatic parenchyma involving more than 50% of the lesion. Additionally, a dynamic pattern of enhancement was defined according to the analysis of the progression of intravenous contrast enhancement (CE) over the progressive different phases of the study, as follows: (1) stable, persistent CE: the nodule enhancement remains invariable through the AP and EP; (2) progressive CE: the nodule enhances progressively over time, reaching maximal intensity in delayed phases; (3) washout: intense contrast uptake during the AP followed by contrast washout in delayed phases. This classification was adopted from Rimola et al²⁶.

The morphologic features of the nodules included the maximum diameter (the IMCCs were categorized according to largest diameter measured on the CT and MRI scans as 3 cm or smaller or larger than 3 cm), the presence of intratumoral calcifications and necrosis at unenhanced phase and T2-weighted images respectively, the contour (round, lobulated, or irregular), the margin (sharp or indistinct), liver surface contour (smooth, bulging or retraction), the presence of small satellite nodules, bile duct dilatation (focal around the lesion or diffuse), the presence of intrahepatic duct stone, vascular and extra-vascular invasion, combined arterioportal shunt, lymph node and distant metastasis and the presence of ascites.

Pathologic Evaluation

Formalin-fixed paraffin embedded liver sections of image-guided percutaneous biopsies or resected specimens were retrospectively reviewed by an experienced liver pathologist who was unaware of the clinical and radiological exams' results. The diagnosis of IMCC was based on morphology, according to standard criteria, and confirmed by immune-histochemical stain

with antibodies against cytokeratin 7 (clone OV-TL-12/30; DAKO Corporation, Carpinteria, CA, USA) and cytokeratin 19 (DAKO-CK19, Code #M888; DAKO A/S, Glostrup, Denmark). Histological differentiation was graded as well-moderately (G1-G2) or poorly differentiated (G3)²⁷. For seven lesions (12.5%), diagnosed by fine needle biopsy, the grade could not be assessed (Gx) because of inadequate cellular component of the tumoral sample. Overall, twenty-nine (51.8%) and 20 (35.7%) cases were well-moderately differentiated and poorly differentiated adenocarcinoma, respectively (Table I).

Statistical Analysis

Categorical variables were compared by twosided Fisher's exact test. Distribution of continuous variables were analyzed for parametric distribution by Kolmogorov-Smirnov test. Since these variables did not show a normal distribution, the association between continuous and categorical variables was assessed by Mann-Whitney U test (for dichotomous variables) and by the Kruskal-Wallis one-way analysis of variance test (for variables with three groups). A conventional *p* value less than 0.05 was considered significant. Data were analyzed with the IBM SPSS Statistic release 22 (SPSS Statistics v22.0, IBM, Chicago, IL, USA).

Results

Morphologic MDCT and MRI Features

The morphologic features of IMCCs are shown in Table II. The median diameter of the lesions was 6.5 cm (range, 1.5-15 cm), and there were 12 (21.4%) IMCCs smaller than or equal to 3 cm in diameter. Intralesional T2 hyperintensity suggestive of intratumoral cystic change or necrosis was noted in 91% of the lesions evaluated by MRI. Lesions contours were most commonly irregular, the hepatic capsule showed a bulging contour in 55.3% of the cases and satellite nodules were found in about one third of the tumours. Bile duct dilatation adjacent to the lesion or diffuse was seen in 15 and 7 nodules, respectively, while lymph node metastasis was noted in 46.4% of the patients.

Enhancement Characteristics

The enhancement patterns of IMCCs in according to AP, PVP and EP are summarized in Table III. All lesions were either hypoattenuat-

Table II. Morphologic MDCT and MRI features of 56 IMCCs.

Feature	Total (n = 56)
Nodule size, median (range), cm	6.5 (1.5-15)
< 3 cm, No. (%)	12 (21.4)
> 3 cm, No. (%)	44 (78.6)
Calcification at MDCT)	5/44 (11.4)
(44 nodules), No. (%	
T2w hyperintensity at MRI	20/22 (91)
(22 nodules), No. (%)	
Contour, No. (%)	
Round	4 (7)
Lobulated	20 (36)
Irregular	32 (57)
Margin, No. (%)	
Sharp	23 (41)
Indistinct	33 (59)
Live surface contour, No. (%)	
Smooth	7 (12.5)
Bulging	31 (55.3)
Retraction	18 (32.2)
Peripheral satellite nodules, No. (%)	21 (37.5)
Intrahepatic duct stone, No. (%)	1 (1.8)
Bile duct dilatation, No. (%)	22 (48)
Focal around the lesion, No. (%)	15 (26.8)
Diffuse, No. (%)	7 (12.5)
Vessel invasion, No. (%)	27 (48)
Extravascular structure invasion, No. (%)	17 (30.3)
Combined arterioportal shunt, No. (%)	2 (3.5)
Lymph node metastasis, No. (%)	26 (46.4)
Distant metastasis, No (%)	2 (3.5)
Ascites, No. (%)	11 (19.6)

ing (97.7%, 43 of 44) or isoattenuating (2.3%, 1 of 44) at MDCT and hypointense (81.8%, 18 of 22), isointense (13.6%, 3 of 22) or hyperintense (4.6%, 1 of 22) at MRI on the T1 weighted-fat suppressed pre-contrast scans. Most of the nodules remained hypoenhancing in all post-contrast phases, respectively 76.8% (43 of 56) on AP, 73.2% (41 of 56) on PVP and 66% (37 of 56) on EP. The lesions were more frequently peripherally hyperenhancing (50%, 28 of 56) on AP, and partially hyperenhancing on PVP (67.9%, 38 of 56) and EP (80.3%, 45 of 56).

Dynamic enhancement patterns displayed by IMCCs are shown in Table IV. The most frequent dynamic pattern displayed by IMCCs was a progressive contrast uptake (82.1%, 46 of 56) (Figure 1). Stable CE (Figure 2) was seen in seven (12.5%) nodules, while 3 (5.4%) nodules showed arterial enhancement with washout (Figure 3), two at MDCT and one at both MDCT and MR images.

Acquisition	Enhancement pattern of tumors						
Phase	Нуј	per	Iso	Нуро			
AP, No. (%) PVP, No. (%) EP, No. (%)	14 (23.2) 25) 28.6)	1 (1.8) 3 (5.4)	43 (76.8) 41 (73.2) 37 (66)			
	Globally Hyper	Partially Hyper	Peripherally Hyper	Iso	Нуро		
AP No. (%)	1 (1.8)	26 (46.4)	28 (50)	_	1 (1.8)		

Table III. MDCT and MRI enhancement patterns of 56 IMCCs in arterial, portal venous, and equilibrium phase.

38 (67.9)

45 (80.3)

AP: arterial phase; PVP: portal venous phase; EP: equilibrium phase; Hyper: hyperenhancing; Iso: isoenhancing; Hypo: hypoenhancing.

16 (28.5)

8 (14.3)

Table IV. MDCT and MRI dynamic enhancement patterns of 56 IMCCs.

1 (1.8)

1(1.8)

PVP, No. (%)

EP, No. (%)

	Stable	Progressive	Washout
Nodules, No. (%)	7 (12.5)	46 (82.1)	3 (5.4)

Tables V and VI show the correlation of presence/absence of chronic liver disease, tumor size, and histological differentiation with arterial and dynamic enhancement patterns, respectively.

1 (1.8)

1 (1.8)

1(1.8)

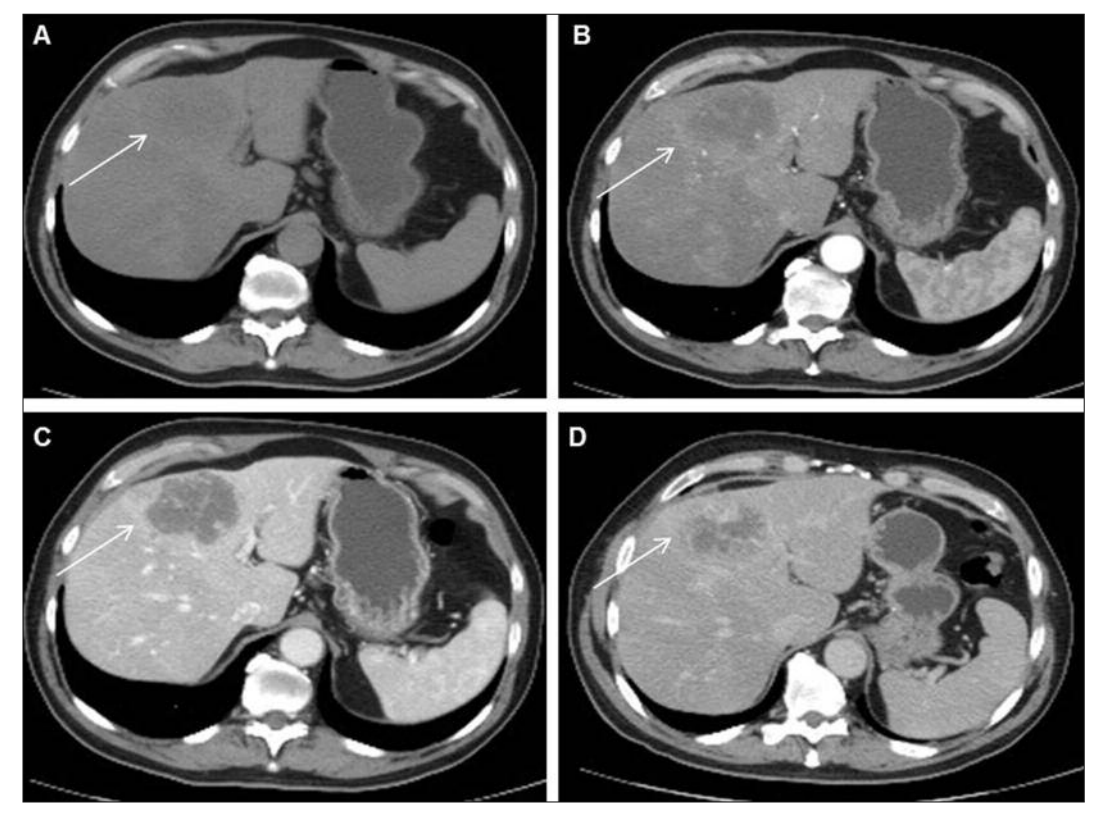


Figure 1. Moderately differentiated IMCC in 69-year old man without chronic liver disease. **A,** Precontrast axial CT image of a 6 cm in diameter nodule in liver IV segment: the nodule is hypodense relative to surrounding liver parenchyma. **B-D,** Axial CT images after non-ionic contrast agent administration. The lesion is peripherally hyperenhancing on **(B)** arterial phase and **(C)** portal venous phases, and it is partially hyperenhancing on (D) equilibrium phase with centripetal and progressive dynamic enhancement pattern.

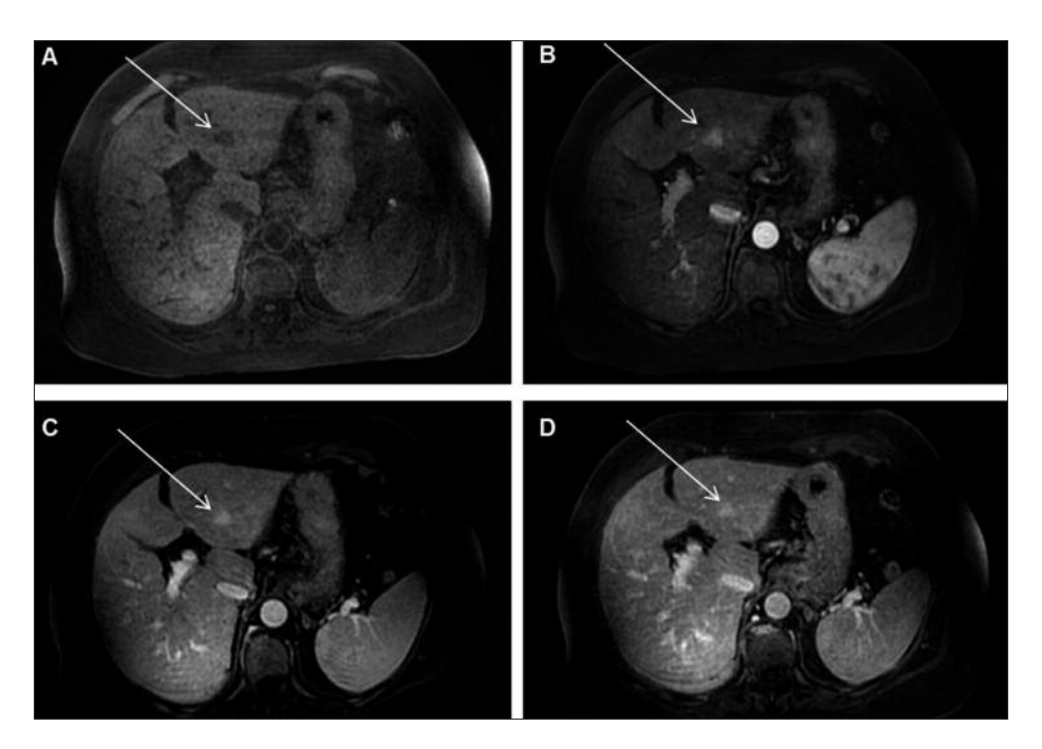


Figure 2. Poorly differentiated IMCC in 64-years old woman with chronic hepatitis due to B-viral infection. **A**, Precontrast axial fat-suppressed T1w 3D SPGR MR image of a 2 cm in diameter nodule in liver III segment: the nodule is hypointense compared with the surrounding liver parenchyma. **B-D**, T1w dynamic 3D SPGR MR images after gadobenate dimeglumine administration. The lesion is globally hyperenhancing on **(B)** arterial, **(C)** portal venous and **(D)** equilibrium phases with stable dynamic enhancement pattern.

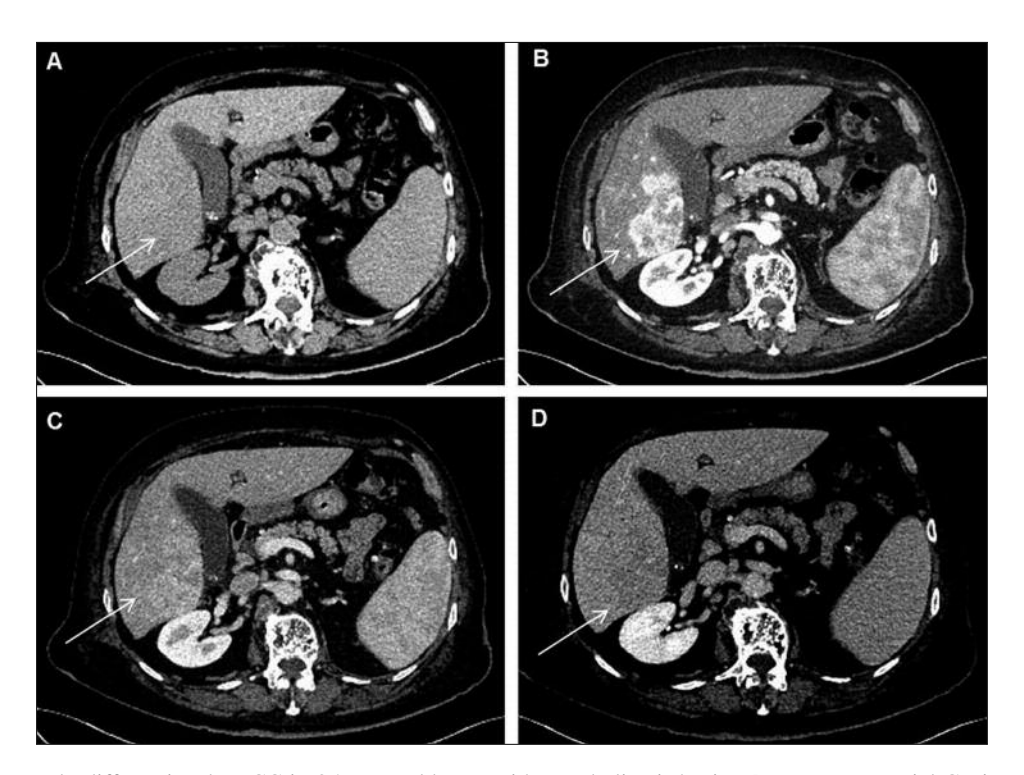


Figure 3. Poorly differentiated IMCC in 85-years old man with metabolic cirrhosis. **A**, Precontrast axial CT image of a 7.5 cm in diameter nodule in liver V and VI segments: the nodule is hypodense relative to surrounding liver parenchyma. **B-D**, Axial CT images after non-ionic contrast agent administration. The lesion is partially hyperenhancing on **(B)** arterial and (C) portal venous phases and shows wash-out enhancement pattern on equilibrium phase **(D)**.

Table V. Correlation between chronic liver disease, tumor size, histological differentiation and arterial enhancement of 56 IMCCs at MDCT and MRI.

	Arterial enhancement of tumors						
Clinicopathological and morphological finding	Hyper (n = 13)	Hypo (n = 43)	p	Globally/ Partially hyper (n = 27)	Peripherally hyper (n = 28)	Hypo (n = 1)	p
Normal liver, No. (%)	6 (46.0)	31 (72)	0.08	19 (70.4)	17 (60.7)	1 (100)	0.58
Chronic liver disease, No. (%)	7 (54.0)	12 (28)		8 (29.6)	11 (39.3)	_	
Nodule size							
Median (range), cm	4.8 (2-14)	7 (1.5-15)	0.11	5.3 (1.8-15)	6.8 (1.5-15)	3	0.6
< 3 cm, No. (%)	5 (38.5)	7 (16.3)	0.09	7 (26)	4 (14.3)	1 (100)	0.09
> 3 cm, No. (%)	8 (61.5)	36 (83.7)		20 (74)	24 (85.7)	_	
Histological differentiation, No. (%)							
Gx	3 (23.0)	4 (9.3)	0.42	4 (14.8)	3 (10.7)	_	0.73
G1-2	6 (46.2)	23 (53.5)		15 (55.6)	13 (46.4)	1 (100)	
G3	4 (30.8)	16 (37.2)		8 (29.6)	12 (42.9)	_	

Gx: grade cannot be assessed; G1-G2: well-moderately differentiated; G3: poorly differentiated; Hyper: hyperenhancing; Hypo: hypoenhancing.

There were not statistically significant differences in arterial enhancement tumors patterns of patients with or without chronic liver disease, whereas dynamic enhancement pattern was significantly correlated to presence/absence of chronic liver disease (p = 0.01). Indeed, progressive CE was significantly more frequent in normal liver (74%, 34 of 46) than in chronic liver disease (26%, 12 of 46), stable CE was found in 4 (57%) IMCCs emerging in chronic liver disease and in 3 IMCCs (43%) emerging in normal liver, while washout CE was observed only in chronic liver disease (100%, 3 of 3, in one patient with chronic B-viral hepatitis, in one pa-

tients with alcohol cirrhosis and in one patient with metabolic cirrhosis, respectively).

There were no significant differences in arterial or in dynamic enhancement patterns in accordance to nodule size (≤ 3 cm and > 3 cm). However, 38 nodules (82.6%) > 3 cm displayed a progressive CE compared to 8 (17.4%) ≤ 3 cm (p = 0.27).

At pathologic examination, histological differentiation showed no significant correlation with arterial enhancement but was significantly related to dynamic enhancement pattern (p = 0.02). IMCCs with progressive CE were more frequently well-moderately differentiated (58.7%, 27 of

Table VI. Correlation between chronic liver disease, tumor size, histological differentiation and dynamic enhancement pattern of 56 IMCCs at MDCT and MRI.

Clinicopathological and morphological finding	Dynamic enhancement pattern of tumors					
	Stable (n = 7)	Progressive (n = 46)	Washout (n = 3)	p		
Normal liver, No. (%) Chronic liver disease, No. (%) Nodule size	3 (43) 4 (57)	34 (74) 12 (26)	0 (.0) 3 (100)	0.01		
Median (range), cm < 3 cm, No. (%) > 3 cm, No. (%)	5 (1.5-15) 3 (43) 4 (57))	6.5 (1.8-15) 8 (17.4) 38 (82.6)	4.8 (3-7.5) 1 (33.3) 2 (66.7)	0.56 0.27		
Histological differentiation, No. (%) Gx G1-2 G3	0 (.0) 1 (14.3) 6 (85.7)	7 (15.2) 27 (58.7) 12 (26.1)	0 (.0) 1 (33.3) 2 (66.7)	0.02		

Gx: grade cannot be assessed; G1-G2: well-moderately differentiated; G3: poorly differentiated.

46); IMCCs with stable CE were more frequently poorly differentiated (85.7%, 6 of 7), while of lesions with washout 2 (66.7%) were poorly and one (33.3%) was well-moderately differentiated.

In addition, there was synchronous nodule of histologically proven HCC in different sites of the liver, in four patients with HBV (n = 2) or HCV (n = 2) related cirrhosis. The HCCs were typically hyperenhancing lesions in AP with washout in EP, while the IMCCs were typically hypoenhancing (peripherally hyperenhancing) lesions in AP with progressive CE in EP.

Discussion

In our study, most of the IMCCs were hypoenhancing and peripherally hyperenhancing in AP and partially hyperenhancing in EP. Then, in agreement with previous studies, the prevalent dynamic enhancement pattern displayed by IM-CCs on 4-MDCT and MRI was a progressive contrast uptake $(82.1\%, 46 \text{ of } 56)^{8-12,19,20,22,26,28}$. However, there were three (5.4%) arterially hyperenhancing lesions, of which two on 4-MDCT images and 1 on both 4-MDCT and MRI, that showed washout in EP. Similar results were reported by other studies of dynamic CT19,20 or MRI^{22,29,30}. Kim et al¹⁹ and Kim et al²⁰ demonstrated that 28.5% (8 of 28) and 4.3% (3 of 70) of IMCCs respectively, showed arterial enhancement with washout during PVP or EP on CT images. Three studies of MRI with gadoxetic acid disodium (Primovist 0.25 mmol/ml; Bayer Schering Pharma AG, Berlin, Germany) reported that 6% (3 of 48)²², 18.75% (6 of 32)²⁹ and 10.5% (2 of 19)31 of IMCCs respectively, showed hyperenhancement on AP with washout in EP. Contradictory findings were noted in a study of MDCT by Iavarone et al²⁸ and in a study of MRI with gadodiamide (Omniscan 0.5 mmol/L; GE Health Diagnostic, Amersham, Madrid, Spain) by Rimola et al²⁶ because both of these studies demonstrated that none of included IMCCs displayed washout at delayed phases. The discrepancy regarding results of MRI studies could be explained by the peculiar characteristic of gadoxetic acid as it is beginning to be taken in hepatocytes about 1 min after intravenous administration. After the AP, PVP and EP images may thus be enhanced by the complex mechanism of combined extracellular persistence and hepatocyte uptake of gadoxetic acid31. However, in our study the lesions with washout were found on 4-MDCT images (three of 3 lesions) and on MR images after intravenous administration of gadobenate dimeglumine (1 of 3 lesions).

We did not find significant differences in arterial enhancement pattern according to presence/absence of underlying chronic liver disease, tumor size and histological differentiation. These results are in agreement with those of a few previous studies regarding the presence of chronic liver disease³⁰, tumor size^{26,28} and histological differentiation^{20,21,30}, respectively. On the other hand, our findings differ from those in other studies, which found much higher incidence of arterially hyperenhancing lesions in patients with chronic liver disease than in patients without^{20,21,23,24}, in the small¹⁹-^{21,24,30} and in the histologically well-differentiated²⁴ IMCCs. This inconsistency can be due to a too small number of arterially hyperenhancing IMCCs in our series (23.2%, 13 of 56).

In our case load, the dynamic enhancement pattern was not related to lesion size, but it appeared to differ significantly in patients with or without chronic liver disease. Progressive CE pattern was more frequently found in normal liver (74%, 34 of 46) than in chronic liver disease (26%, 12 of 46), whereas washout was observed only in IMCCs emerging in chronic liver disease (100%, 3 of 3) (p = 0.01). These findings correspond partially with those of the three previous studies that investigated the ICCs features on dynamic CT19,28 or MRI26 in cirrhotic patients and correlated the temporal changes of enhancement with tumor size. Kim et al¹⁹ found the enhancement pattern of ICCs in cirrhotic liver to differ depending on tumor size at CT imaging; a washout pattern on PV scans was the most frequent (five of 8 cases) in nodules smaller than 3 cm in diameter and there was no significant difference between the enhancement pattern of ICC and that of HCC, while peripheral or centripetal enhancement pattern was the most frequent (9 of 20 cases) in tumors larger than 3 cm, resembling the classic CT findings of ICC in normal hepatic parenchyma. However, in this study, only AP and PVP were described, omitting the valuable information of EP. Subsequently, Rimola et al²⁶ demonstrated that the most characteristic MRI contrast pattern of ICC in cirrhosis was a progressive contrast uptake throughout the different phases (80.6%, 25 of 31 lesions), whereas contrast washout at EP was not observed. The dynamic behavior differed significantly according to tumor size: progressive enhancement pattern was the most frequent in lesions larger than 2 cm (20 of 25 cases), whereas the stable pattern was mainly identified in nodules smaller than 2 cm (4 of 6 cases). Recently, Iavarone et al²⁸ assessed the temporal changes of 40 IMCCs during contrast enhanced 4-MDCT-scan in the setting of cirrhosis in relation to the nodule size. The most frequent dynamic pattern was a progressive homogeneous contrast uptake (42%, 16 of 40 cases), without relation to tumor size and a contrast washout at EP was not observed.

In clinical practice, the nodules with stable CE may be regarded as indeterminate nodules and a biopsy should be mandatory for diagnosis, while arterially hypervascular lesions with washout in EP found in chronic liver disease, could be misdiagnosed as HCCs. This misdiagnosis may result in the inappropriate selection for different treatment strategies, because surgical resection is the treatment of choice for IMCC15, while various kinds of treatment methods (e.g., surgical resection, liver transplantation, and percutaneous or trans arterial local ablation) can be used for HCCs¹⁴. Therefore, according to our study findings and those of other experiences that found arterially hypervascular IMCCs with wash-out in EP on MDCT and MRI scans, the current non-invasive diagnostic criteria for HCC13,14 could be questioned.

Interestingly, Park et al²⁹ enrolled sixty-four patients with pathologically proven small (≤ 3 cm) IMCCs (n = 32) and HCCs (n = 32) who underwent preoperative gadoxetic acid-enhanced MRI and diffusion-weighted imaging (DWI). Multivariate logistic regression analysis revealed that target appearance on the DWI was a significant and independent variable predictive of IM-CC, because 24 IMCCs (75%) and only one (3.1%) scirrhous HCC showed this feature (p =0.0003). The authors speculated that the presence of loose fibrosis with edema might be responsible for the DWI and HBP target appearance. In our opinion, further studies are needed to assess if the addition of DWI may improve the effectiveness of contrast enhanced MRI in the differential diagnosis between IMCC and HCC emerging in liver cirrhosis.

In addition, in our radiologic-pathologic correlation, we found that progressive CE was more frequently showed by well-moderately differentiated IMCCs (58.7%, 27 of 46 cases) than by poorly differentiated IMCCs (26.1%, 12 of 46 cases), stable CE was more frequently displayed in poorly differentiated lesions (85.7%, 6 of 7 cases), while regarding contrast washout 2 IM-

CCs were poorly differentiated and one nodule was well-moderately differentiated (p = 0.02). To the best of our knowledge, no previous studies correlated dynamic pattern of IMCC at 4-MDCT or dynamic MRI with histological differentiation. Our findings suggest that well-moderately differentiated lesions more frequently display typical dynamic pattern of IMCC, while poorly differentiated lesions can show indeterminate pattern or contrast wash-out as nodules of HCC. This might support the hypothesis of common cell ancestors to IMCC and HCC⁶.

Interestingly, in our series there were four patients with HBV-related (2 cases) or HCV-related (2 cases) cirrhosis and synchronous incidental HCC associated with one nodule of IMCC in different sites of the liver. The prevalence of synchronous development of double hepatic primary cancer is estimated to be 0.25% of the primary liver cancers³². Even though the biomolecolar and clinicopathological features of this phenomenon have not been clarified, recent studies suggest a relationship between HCV and/or HBV infection and risk of double primary hepatic tumor^{32,34}. Our results confirm the close relationship between IMCC and HCC, which could originate from the same hepatic progenitor stem cells in patients with chronic liver disease⁶.

This study was retrospective and this implies the potential possibility of selection bias. However, our report provides a relatively large series of pathologically confirmed IMCCs seen at 4-MD-CT or dynamic MRI. Moreover, the number of IMCCs in chronic liver disease was smaller than those in normal hepatic parenchyma, but these findings reflect the lower prevalence of IMCCs in patients with chronic liver disease that in those without. Finally, radiologic-pathologic correlation was possible in only 49 lesions as in 7 biopsy-proven IMCCs the assessment of tumour grading was not possible.

Conclusions

The most prevalent enhancement pattern of IMCCs on 4-MDCT and enhanced MR images was initial rim enhancement in AP, followed by progressive and concentric filling. The stable and washout pattern were more frequent in poorly differentiated IMCCs. In chronic liver disease some IMCCs displayed a washout pattern indistinguishable from that of typical HCC.

Conflict of Interest

The Authors declare that there are no conflicts of interest.

References

- PATEL T, SINGH P. Cholangiocarcinoma: emerging approaches to a challenging cancer. Curr Opin Gastroenterol 2007; 23: 317-323.
- European HPB Association Consensus Conference on Cholangiocarcinoma. HPB 2008; 2: 71-147.
- YANG JD, KIM B, SANDERSON SO, SAUVER J, YAWN BP, LARSON J, THERNEAU TM, ROBERTS LR, GORES GJ, KIM WR. Biliary tract cancers in Olmsted County, Minnesota, 1976-2008. Am J Gastroenterol 2012; 107: 1256-1262.
- 4) ZHOU Y, ZHAO Y, LI B, HUANG J, WU L, XU D, YANG J, HE J. Hepatitis viruses infection and risk of intrahepatic cholangiocarcinoma: evidence from a meta-analysis. BMC Cancer 2012; 12: 289-295.
- PALMER WC, PATEL T. Are common factors involved in the pathogenesis of primary liver cancers? A meta-analysis of risk factors for intrahepatic cholangiocarcinoma. J Hepatol 2012; 57: 69-76.
- 6) OISHI N, KUMAR MR, ROESSLER S, JI J, FORGUES M, BUDHU A, ZHAO X, ANDERSEN JB, QH, JIA HL, QIN LX, YAMASHITA TH, HG WOO, KIM YJ, KANEKO S, TANG ZY, THORGEIRSSON SS, WANG XW. Transcriptomic profiling reveals hepatic stem-like gene signatures and interplay of miR-200c and epithelial-mesenchymal transition in intrahepatic cholangio-carcinoma. Hepatology 2012; 56: 1792-1803.
- LIVER CANCER STUDY GROUP OF JAPAN. Classification of primary liver cancer. Tokyo, Japan: Kanehara, 1997; pp. 6-8.
- SOYER P, BLUEMKE DA, REICHLE R, CALHOUN PS, BLISS DF, SCHERRER A, FISHMAN EK. Imaging of intrahepatic cholangiocarcinoma: 1. Peripheral cholangiocarcinoma. Am J Roentgenol 1995; 165: 1427-1431.
- LACOMIS JM, BARON RL, OLIVER JK, NALESNIK MA, FEDERLE MP. Cholangiocarcinoma: delayed CT contrast enhancement patterns. Radiology 1997; 203: 98-104.
- KIM TK, CHOI BI, HAN JK, CHO SG, HAN MC. Peripheral cholangiocarcinoma of the liver: two-phase spiral CT findings. Radiology 1997; 204: 539-543.
- LOYER EM, CHIN H, DUBROW RA, DAVID CL, EFTEKHARI F, CHARNSANGAVEJ C. Hepatocellular carcinoma and intrahepatic peripheral cholangiocarcinoma: enhancement patterns with Quadruple Phase Helical CT--A Comparative Study. Radiology 1999; 212: 866-875.
- MAETANI Y, ITOH K, WATANABE C, AMETANI F, YAMABE H, KONISHI J. MR imaging of intrahepatic cholangiocarcinoma with pathologic correlation. Am J Roentgenol 2001; 176: 1499-1507.

- BRUIX J, SHERMAN M. American Association for the Study of Liver Disease (AASLD). Management of hepatocellular carcinoma: an update. Hepatology 2011; 53: 1020-1022.
- 14) EUROPEAN ASSOCIATION FOR THE STUDY OF THE LIVER, EUROPEAN ORGANISATION FOR RESEARCH AND TREATMENT OF CANCER. EASL-EORTC clinical practice guidelines: management of hepatocellular carcinoma. J Hepatol 2012; 56: 908-943.
- BRIDGEWATER J, GALLE PR, KHAN S, LLOVET JM, PARK JW, PATEL T, PAWLIK TM, GORES GJ. Guidelines for the diagnosis and management of intrahepatic cholangiocarcinoma. J Hepatol 2014; 60: 1268-1289.
- 16) CHONG YS, KIM YK, LEE MW, KIM SH, LEE WJ, RHIM HC, LEE SJ. Differentiating mass-forming intrahepatic cholangiocarcinoma from atypical hepatocellular carcinoma using gadoxetic acid-enhanced MRI. Clin Radiol 2012; 67: 766-773.
- 17) VILANA R, FORNER A, BIANCHI L, GARCÍA-CRIADO A, RI-MOLA J, DE LOPE CR, REIG M, AYUSO C, BRÚ C, BRUIX J. Intrahepatic peripheral cholangiocarcinoma in cirrhosis patients may display a vascular pattern similar to hepatocellular carcinoma on contrast-enhanced ultrasound. Hepatology 2010; 51: 2020-2029.
- 18) GALASSI M, IAVARONE M, ROSSI S, BOTA S, VAVASSORI S, ROSA L, LEONI S, VENERANDI L, MARINELLI S, SANGIO-VANNI A, VERONESE L, FRAQUELLI M, GRANITO A, GOLFIERI R, COLOMBO M, BOLONDI L, PISCAGLIA F. Patterns of appearance and risk of misdiagnosis of intrahepatic cholangiocarcinoma in cirrhosis at contrast enhanced ultrasound. Liver Int 2013; 33: 771-779.
- KIM SJ, LEE JM, HAN JK, KIM KH, LEE JY, CHOI BI. Peripheral mass-forming cholangiocarcinoma in cirrhotic liver. Am J Roentgenol 2007; 189: 1428-1434.
- 20) KIM SA, LEE JM, LEE KB, KIM SH, YOON SH, HAN JK, CHOI BI. Intrahepatic mass-forming cholangiocarcinomas: enhancement patterns at multiphasic CT, with special emphasis on arterial enhancement pattern-correlation with clinicopathologic findings. Radiology 2011; 260: 148-157.
- ARIIZUMI SI, KOTERA Y, TAKAHASHI Y, KATAGIRI S, CHEN IP, OTA T, YAMAMOTO M. Mass-forming Intrahepatic Cholangiocarcinoma with marked enhancement on arterial-phase computed tomography reflects favorable surgical outcomes. J Surg Oncol 2011; 104: 130-139.
- KANG Y, LEE JM, KIM SH, HAN JK, CHOI BI. Intrahepatic mass-forming cholangiocarcinoma: enhancement patterns on gadoxetic acid-enhanced MR images. Radiology 2012; 264: 751–760.
- 23) Xu J, Igarashi S, Sasaki M, Matsubara T, Yoneda N, Kozaka K, Ikeda H, Kim J, Yu E, Matsui O, Nakanuma Y. Intrahepatic cholangiocarcinomas in cirrhosis are hypervascular in comparison with those in normal livers. Liver Int 2012; 32: 1156-1163.
- 24) Nanashima A, Abo T, Muratami G, Matsumoto A, Tou K, Takeshita H, Kunizaki M, Hidaka S, Sakamoto

- I, HAYASHI H, FUKUDA T, KUDO T, NAGAYASU T. Intrahepatic cholangiocarcinoma: relationship between tumor imaging enhancement by measuring attenuation and clinicopathologic characteristics. Abdom Imaging 2013; 38: 785-792.
- 25) BOLL DT, MERKLE EM. Diffuse liver disease: strategies for hepatic CT and MR imaging. Radiographics 2009; 29: 1591-1614.
- 26) RIMOLA J, FORNER A, REIG M, VILANA R, DE LOPE CR, AYUSO C, BRUIX J. Cholangiocarcinoma in cirrhosis: absence of contrast washout in delayed phases by magnetic resonance imaging avoids misdiagnosis of hepatocellular carcinoma. Hepatology 2009; 50: 791-798.
- EDGE S, BYRD D, COMPTON C. AJCC Cancer Staging Manual. 7th ed. New York: Springer-Verlag, 2010: 201-09.
- 28) IAVARONE M, PISCAGLIA F, VAVASSORI S, GALASSI M, SAN-GIOVANNI A, VENERANDI L, FORZENIGO LV, GOLFIERI R, BOLONDI L, COLOMBO M. Contrast enhanced CT-scan to diagnose intrahepatic cholangiocarcinoma in patients with cirrhosis. J Hepatol 2013; 58: 1188-1193.
- PARK HJ, KIM YK F, PARK MY, LEE WJ. Small intrahepatic mass-forming cholangiocarcinoma: target sign on diffusion-weighted imaging for differentiation from hepatocellular carcinoma. Abdom Imaging 2013; 38: 793-801.
- 30) KIM SH1, LEE CH, KIM BH, KIM WB, YEOM SK, KIM KA, PARK CM. Typical and atypical imaging find-

- ings of intrahepatic cholangiocarcinoma using gadolinium ethoxybenzyl diethylenetriamine pentaacetic acid-enhanced magnetic resonance imaging. J Comput Assist Tomogr 2012; 36: 704-709.
- 31) JEONG HT, KIM MJ, CHUNG YE, CHOI JY, PARK YN, KIM KW. Gadoxetate disodium-enhanced MRI of mass-forming intrahepatic cholangiocarcinomas: limaging-histologic correlation. Am J Roentgenol 2013; 20: 603-611
- 32) TAMADA T, ITO K, SONE T, YAMAMOTO A, YOSHIDA K, KAKUBA K, TANIMOTO D, HIGASHI H, YAMASHITA T. Dynamic contrast-enhanced magnetic resonance imaging of abdominal solid organ and major vessel: comparison of enhancement effect between Gd-EOB-DTPA and Gd-DTPA. J Magn Reson Imaging 2009; 29: 636-640.
- 33) CAO J, HUANG L, LIU C, LI J, ZHANG X, SHEN J, LI J, LU L, XU F, YAN J, WU M, LAU WY, YAN Y. Double primary hepatic cancer (hepatocellular carcinoma and intrahepatic cholangiocarcinoma) in a single patient: a clinicopathologic study of 35 resected cases. J Gastroenterol Hepatol 2013; 28: 1025-1031.
- 34) INABA K, SUZUKI S, SAKAGUCHI T, KOBAYASI Y, TAKEHARA Y, MIURA K, BABA S, NAKAMURA S, KONNO H. Double primary hepatic cancer (intrahepatic cholangio-carcinoma and hepatocellular carcinoma) in a patient with hepatitis C virus-related cirrhosis. J Hepatobiliary Pancreat Surg 2007; 14: 204-209.